

# Measurement of the spatial resolution and the relative density resolution in an industrial cone-beam micro computed tomography system

WANG Yan-Fang(王燕芳)<sup>1,2</sup> QUE Jie-Min(阙介民)<sup>1,2</sup> CAO Da-Quan(曹大泉)<sup>1,2,3</sup> SUN Cui-Li(孙翠丽)<sup>1,2</sup>  
ZHAO Wei(赵维)<sup>1,2,3</sup> WEI Cun-Feng(魏存峰)<sup>1,2</sup> SHI Rong-Jian(史戎坚)<sup>1,2</sup> WEI Long(魏龙)<sup>1,2</sup>

<sup>1</sup> Key Laboratory of Analytical Techniques, Institute of High Energy Physics, Chinese Academy of Sciences, Beijing 100049, China

<sup>2</sup> Beijing Engineering Research Center of Radiographic Techniques and Equipment, Beijing 100049, China

<sup>3</sup> University of Chinese Academy of Sciences, Beijing 100049, China

**Abstract:** The spatial resolution and the relative density resolution are the two most critical indicators in CT system. The method recommended in the ASTM E1695-95 and GJB 5311-2004 is only suitable to the fan-beam CT system. In this paper, for industrial cone-beam micro CT system, we will adopt the edge response function (ERF) created by the step edges of a steel ball to measure the system 3D PSF and MTF. To describe the contrast discrimination function more accurately, we will first propose to extend the two-dimensional measurement region to the three-dimensional space. Our experimental spatial resolution is  $(55.56 \pm 0.56)$  lp/mm and the relative density resolution is 1% within  $300 \mu\text{m} \times 300 \mu\text{m} \times 300 \mu\text{m}$  according to the  $3\sigma$  rule.

**Key words:** micro computed tomography, point spread function, contrast discrimination function, modulation transfer function

**PACS:** 81.70.Tx, 02.50.-r, 29.85.Ca **DOI:** 10.1088/1674-1137/37/7/078202

## 1 Introduction

An industrial cone-beam micro computed tomography system (ICB $\mu$ CT) includes an X-ray tube with micro focal spot, a precision turntable, a flat panel detector, and a cone-beam reconstruction algorithm. Compared with an industrial fan-beam computed tomography system, it has the advantages of a high X-ray utilization rate, short data acquisition time, and high isotropy resolution, so ICB $\mu$ CT is a genuine three-dimensional (3D) imaging system. For evaluating a CT system, the two main factors are the spatial resolution, which is defined as the ability of identifying and distinguishing the small detailed features, and the relative density resolution, which is defined as the ability of distinguishing two kinds of materials density. These two indicators basically determine the maximum details resolution of objects and the minimum density difference of materials in a CT system.

The spatial resolution is commonly shown as the degree of a point object to be blurred in imaging process, and described as the point spread function (PSF) or the modulation transfer function (MTF: the modulus of the Fourier transformed PSF). The system PSF is determined by the focal spot size, the detector cell size,

the precision of volume reconstruction algorithm [1] and so on, so it is difficult to derive a formula to define the system PSF accurately. However, it can be measured by experiments. There are two kinds of standard to describe how to measure the system PSF exactly. One is the ASTM (American Society for Testing and Materials) standard E1695-95 [2], the other is the NMS (National Military Standard) GJB 5311-2004 [3]. However, these methods are more suitable for the fan-beam CT system, and not for the cone-beam  $\mu$ CT system. In the cone-beam system, only by obtaining the 3D PSF can we characterize the spatial resolution more accurately.

The 3D PSF can be measured by different experimental methods.

1) Using the point spread of an ideal point object imaged to measure the system PSF, in fact, a micro and exact point object is difficult to manufacture. Moreover, according to the GJB 5311-2004[3], the PSF function should be fitted by a number of points which can not be generated in a micro CT system because of the micro point phantom. So this method is seldom put into practice.

2) To overcome the pitfalls of the previous method, we can use the edge response function (ERF) created by the step edges of a phantom to measure the system PSF

Received 31 August 2012, Revised 6 November 2012

©2013 Chinese Physical Society and the Institute of High Energy Physics of the Chinese Academy of Sciences and the Institute of Modern Physics of the Chinese Academy of Sciences and IOP Publishing Ltd

(the PSF is the first derivative of the ERF). Zikuan Chen [4] used small teflon balls (diameter  $\sim 4.8$  mm) to calculate the full-width-at-half-maximum (FWHM) of the PSF in three planes, which is considered as the spatial resolution of the cone-beam 3D CT imaging system. The result is that the FWHM is  $0.65 \pm 0.08$  mm at the space position (0,0,0). His method is more applicable to the medical CT system. The ICB $\mu$ CT system requires achieving a higher level resolution of  $\mu\text{m}$ .

3) The other one is the linepairs measurement method. It is widely used in the industrial fan-beam computed tomography system. The spatial resolution is the 10% MTF value obtained in linepairs CT images [5]. But, the linepairs phantom for the ICB $\mu$ CT system is not available.

The relative density resolution which is described as the ability to distinguish two kinds of materials density (or the linear attenuation coefficient), not only related with the absorption coefficient difference of two materials, but also influenced by the spatial resolution, noise, the shape and size of the object details, is usually defined as the contrast discrimination function (CDF) within a certain region. The measurement method recommended by the United States ASTM Standard E1695-95 [2] and the GJB 5311-2004 [3] is only for the fan-beam CT system, the relative density resolution obtained by one slice is clearly not applicable to the three-dimensional cone-beam  $\mu$ CT system. At present, the method of measuring the relative density resolution for the cone-beam  $\mu$ CT system is not yet published.

In this paper, for the cone-beam  $\mu$ CT system, we will

$$\begin{aligned}
 g(x,y,z;x_0,y_0,z_0) &= \iiint_{\Omega(x_0,y_0,z_0)} f(x',y',z')h(x-x',y-y',z-z';x_0,y_0,z_0)dx'dy'dz'+n(x,y,z) \\
 &= f(x,y,z)***h(x,y,z;x_0,y_0,z_0)+n(x,y,z) \\
 \forall(x,y,z) &\in \Omega(x_0,y_0,z_0),
 \end{aligned}
 \tag{2}$$

where the position  $(x_0,y_0,z_0)$  denotes a 3D space point in a local region. For a linear spatial invariant system, the 3D PSF is decomposed into three two-dimensional PSFs (2D PSFs) at three orthogonal planes as denoted by the subscripts  $\{x,y,z\}$  [6]. So the 3D to 2D decomposition is expressed by Eq. (3)

$$h(x,y,z)=h_x(y,z)h_y(x,z)h_z(x,y). \tag{3}$$

To sum up, measuring the system 3D PSF exactly, we can utilize three 2D PSFs at three orthogonal planes ( $x$ - $y$  plane,  $y$ - $z$  plane and  $x$ - $z$  plane). It is implemented efficiently and needs less calculation work. Introduced in Part One, the microphantom-based PSF measurement suffers from some pitfalls due to its dependence on the point phantom size and accuracy, so researchers [1, 4, 6,

adopt the second method to measure the system 3D PSF and MTF by using the ERFs of a steel ball. To describe the contrast discrimination function more accurately, we will firstly propose to extend the two-dimensional measure region to the three-dimensional space.

## 2 Methodology

### 2.1 The measurement of the 3D PSF in the ICB $\mu$ CT system

#### 2.1.1 3D PSF and its decomposition

For a CT imaging system, considering the 3D analog object as the input  $f(x,y,z)$ , the reconstructed volume as the output  $g(x,y,z)$ , the relationship between the input and the output are shown in Fig. 1 and Eq. (1).

$$g(x,y,z)=f(x,y,z)***h(x,y,z)+n(x,y,z), \tag{1}$$

where \*\*\* represents the triple convolution,  $h(x,y,z)$  denotes the system 3D PSF and  $n(x,y,z)$  is the additive noise caused by various factors. For a spatial variant system, if the variance over the object support region changes slowly and smoothly, the convolution formula in Eq. (1) approximately holds for a local region [4]. So Eq. (1) can be expressed by Eq. (2):

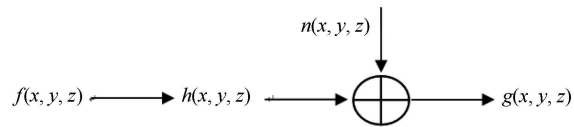


Fig. 1. The diagram of a CT imaging system.

7] obtained the 3D PSF by ERF indirectly.

#### 2.1.2 ERF and its characteristic

An ideal edge is composed of a series of pixels with gray  $h_1$  and a series of pixels with gray  $h_2$ , expressed in Eq. (4), which is provided by a geometrical object with a step edge. After the image blurring of the step edge, the blurred edge profile is called ERF, as illustrated in Fig. 2(a). According to the experimental results, it is reasonable to model the PSF by a Gaussian shape as given by Eq. (5) and Fig. 2(b)

$$f(x)=\begin{cases} h_1 & x \leq x_0 \\ h_2 & x > x_0 \end{cases}, \tag{4}$$

$$h(x)=\frac{1}{(2\pi)^{1/2}\sigma}e^{-\frac{x^2}{2\sigma^2}}. \tag{5}$$

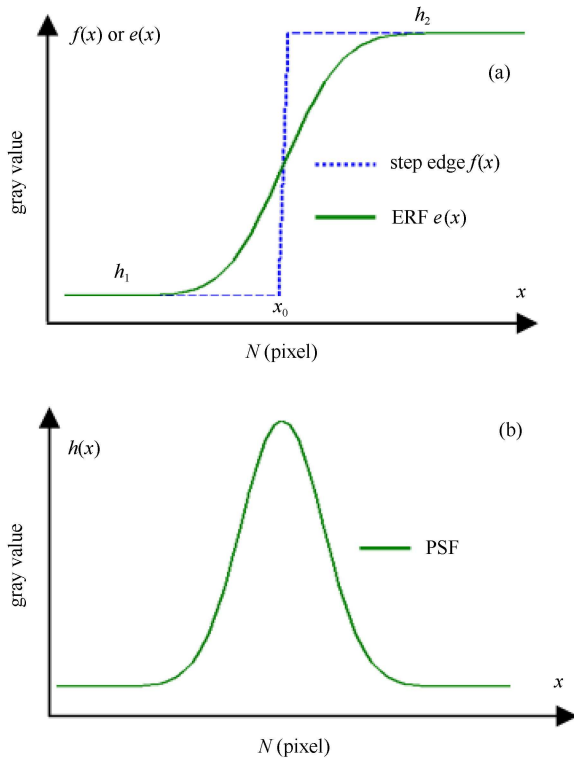


Fig. 2. (a) Step edge and ERF; (b) PSF with a Gaussian shape.

Mathematically, the PSF is the first derivative of the ERF and the MTF is the Fourier transform of the PSF. The relationship among PSF, ERF and MTF is shown in Fig. 3.

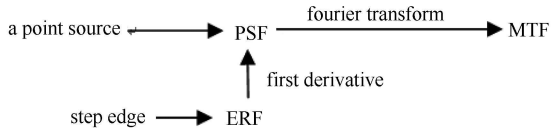


Fig. 3. The relationship among PSF, ERF and MTF.

### 2.1.3 3D PSF and MTF measurement

We extract three orthogonal axial slices from the reconstructed volume data of a steel ball. In each slice, the

radial profiles can be generated as many times as possible. A rising edge or falling edge in each profile is called ERF. PSF is the first derivative of ERF and MTF is the Fourier transform of PSF.

The measuring procedures are as follows.

1) Extracting three orthogonal axial slices at the ball center: transaxial slice ( $x$ - $y$  plane:  $z=0$ ), coronal slice ( $x$ - $z$  plane:  $y=0$ ), sagittal slice ( $y$ - $z$  plane:  $x=0$ ), as shown in Fig. 4 (a), (b).

2) Adding 18 sets of ERF profiles generated by radial scanlines with a  $10^\circ$  increment in each slice, as shown in Fig. 4 (c), we can obtain the average ERF profile.

3) Adding 54 sets of ERF profiles generated by radial scanlines with a  $10^\circ$  increment in three orthogonal axial slices, we can obtain the average ERF profile. The 3D PSF is the first derivative of the average ERF profile and the MTF which is the modulus of the Fourier transformed 3D PSF is regarded as the spatial resolution of the ICB $\mu$ CT system.

4) Generating 18 sets of ERF profiles that are different from the previous samples, we repeat Step 2) and 3). The exact system spatial resolution (10% MTF value) and error level are given.

## 2.2 The measurement of the 3D CDF in the ICB $\mu$ CT system

### 2.2.1 Conventional two-dimensional density resolution measurement

For the fan-beam CT system, the uniform disc method is recommended in the GJB 5311-2004 [3]. When the uniform disc is scanned, it should be placed in the center of a mechanically turntable stage, the rotating axis is perpendicular to the plane of the scanning slice. Within the central region of the disc CT images, a series of block models ranging in size from a single pixel to  $n^2$  pixels are chosen, as shown in Fig. 5. The mean gray value within each block for each type of block size is calculated. The standard deviation in the mean of the certain block size is obtained by calculating the standard deviation. With the increase of the block size, the relationship between the block size and the standard deviation in the mean is established.



Fig. 4. Sampling of the ERF. (a) The three orthogonal slices; (b) the  $x$ - $y$  plane; (c) the ERF profiles.

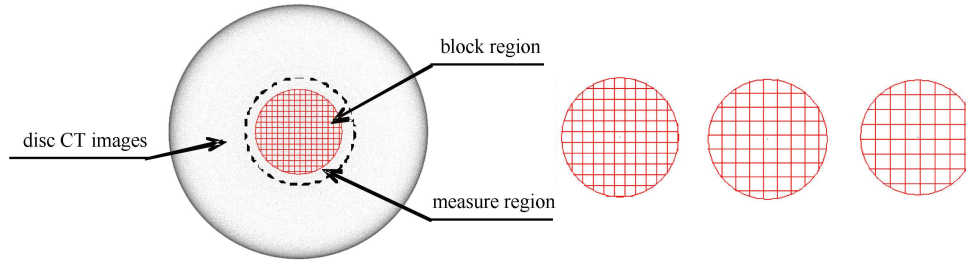


Fig. 5. The two-dimensional measurement region of relative density resolution.

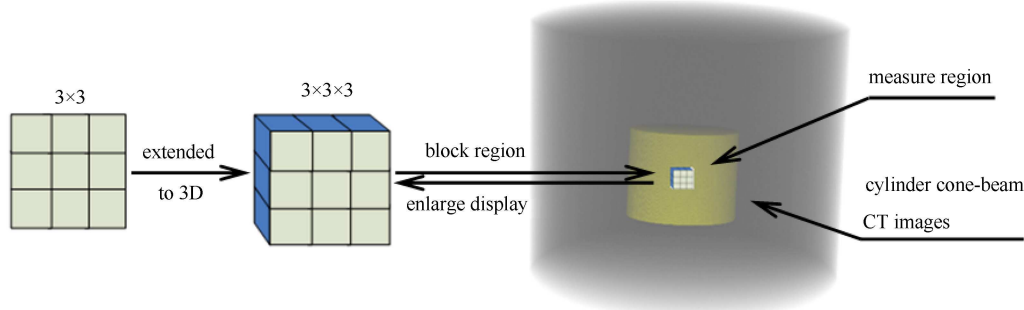


Fig. 6. The measurement region extended from a two-dimensional region to a three-dimensional region.

From above method it can be seen that the different size blocks selected in two-dimensional CT images can be used to reflect the density resolution of the fan-beam CT system, but it is obviously not suitable for the three-dimensional cone-beam  $\mu$ CT system. It is necessary to extend the sampling range from two-dimensional space to three-dimensional space to accurately describe the density resolution of the 3D cone-beam  $\mu$ CT system.

### 2.2.2 The density measurement of the 3D cone-beam $\mu$ CT system

This paper will refer to the GJB method on the measurement of the relative density resolution and extend it to three-dimensional space.

#### 2.2.2.1 The method overview

When scanning the uniform cylindrical standard object in a 3D cone-beam  $\mu$ CT, the transaxial plane should be perpendicular to the flat panel detector. From the cone-beam  $\mu$ CT images, we select a series of block models which fit within the central region of the cylinder. The block size is extended from  $n^2$  pixels to  $n^3$  pixels as shown in Fig. 6. For each type of block size, we calculate the mean gray value within each block and the standard deviation to obtain the standard error in the mean. With the increase of the block size, the relationship between the block size and the standard error in the mean is established. We express each standard error in the mean as a percentage of its respective ensemble average and multiply by a factor of 3 to obtain the contrast discrimination function (CDF) that actually is the den-

sity resolution in the 3D cone-beam  $\mu$ CT system.

#### 2.2.2.2 The measurement region range

The measurement region range should be large enough to encompass a statistically significant number of blocks, but not so large that the cupping artifacts will influence the measurement result [2, 3]. Referring to the GJB 5311-2004 [3], the measurement region volume is about one third of the cylinder as shown in Fig. 6.

#### 2.2.2.3 The block size range

The measurement region is divided into equal size and non-overlapping blocks. The unit of the block is a voxel. The block size range is from a single voxel to  $n$  (the maximum size referring to GJB 5311-2004 [3] provisions) voxels. Different sizes of block models are formed.

#### 2.2.2.4 Calculation of the standard deviation in the mean

- 1) Selecting the measurement region and the block model
- 2) Calculating the mean gray value within each block for each type of block size, the ensemble average is obtained.
- 3) Calculating the standard deviation to obtain the standard deviation in the mean.

#### 2.2.2.5 Generation of the CDF curve

- 1) Establishing the relationship between the block size and the standard deviation in the mean in the order of ascending block size.
- 2) Expressing each standard deviation in the mean as a percent of its respective ensemble average and multiplied by a factor of 3 to obtain the CDF curve.
- 3) Plotting the CDF curve in logarithmic coordinates,

which can read out the relative density resolution in different region sizes.

### 3 Experiment

#### 3.1 The experimental conditions

The experiment has been carried out on a 225 kVp cone-beam  $\mu$ CT system developed by the Institute of High Energy Physics (IHEP), Chinese Academy of Sciences (CAS). The system is equipped with an Phoenix xs-225d X-ray tube (GE, USA) with the 5–15  $\mu$ m focal spot size, Huber 410A turntable (Huber, Germany) and CsI flat panel detector (PaxScan 4030CB, Varian Medical System, UT, USA) which has a pixel (194  $\mu$ m) array 2048 $\times$ 1536. We choose a steel ball (diameter  $\sim$ 500  $\mu$ m)

as the phantom to measure the system PSF and a Poly-methylMethacrylate (PMMA) cylinder as the phantom to measure the system CDF. The experimental settings are listed in Table 1.

#### 3.2 Data processing

##### 3.2.1 Data processing of the spatial resolution measurement

After correcting the beam hardening artifacts, we obtain 182 layers  $\mu$ CT slices with the Feldkamp-Davis-Kress (FDK) volume reconstruction [8]. The 2D cross sectional images are extracted on three principal axial slices across the center of steel ball. The 3D view of the steel ball and three orthogonal axial slices are shown in Fig. 7. The edges of three slices detected by the Canny algorithm [9] are presented in Fig. 8.

Table 1. The experimental settings.

system parameters	spatial resolution experiment	density resolution experiment
X-ray source	120 kV, 40 uA	160 kV, 440uA
flat panel detector	397 mm $\times$ 298 mm, 1fps	397 mm $\times$ 298 mm, 3fps
gantry radius	5 mm	27 mm
source-detector distance	1206 mm	1206 mm
source-object distance	17 mm	165 mm
projection number	1800	1800
reconstruction volume array	2048 $\times$ 2048 $\times$ 1536	2048 $\times$ 2048 $\times$ 1536
voxel	2.74 $\mu$ m $\times$ 2.74 $\mu$ m $\times$ 2.74 $\mu$ m	26.7 $\mu$ m $\times$ 26.7 $\mu$ m $\times$ 26.7 $\mu$ m
cone-beam reconstruction algorithm	feldkamp	feldkamp
cone-beam angle	$\pm 7^\circ$	$\pm 9^\circ$
object	steel ball: $\sim \phi 0.5$ mm	PMMA: $\phi 50$ mm

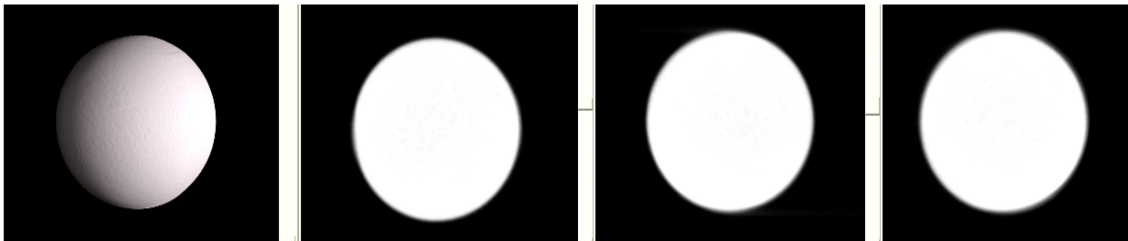


Fig. 7. The 3D view of the steel ball and three orthogonal axial slices.

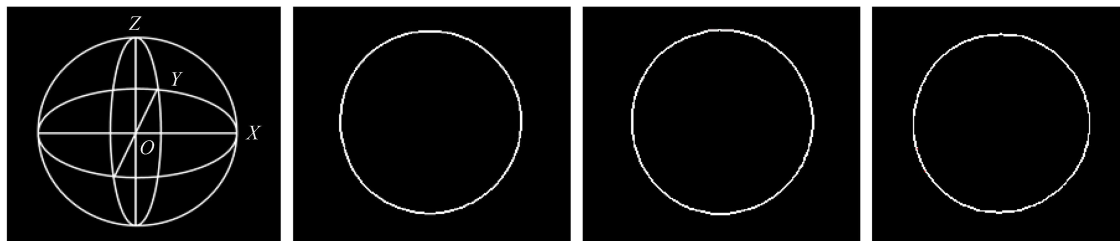


Fig. 8. The edges of the three orthogonal axial slices.

We measure the system PSF through the steel ball volume data, so the ball roundness and surface finish are very important for measurement accuracy. The average radius of steel ball is obtained by the least square method, the root-mean-square (RMS) error of the radius is calculated by 1544 edge points in three orthogonal slices. The result is given by Eq. (6) and presented in Fig. 9

$$R_{\text{ball}} = (90.82 \pm 0.58) \text{ pixels}$$

$$= (248.85 \pm 1.59) \mu\text{m}.$$

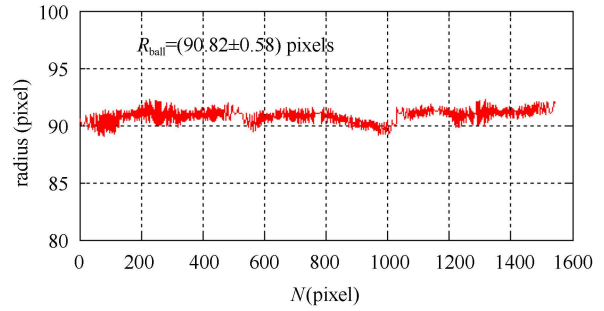


Fig. 9. The average and RMS error of the ball radius.

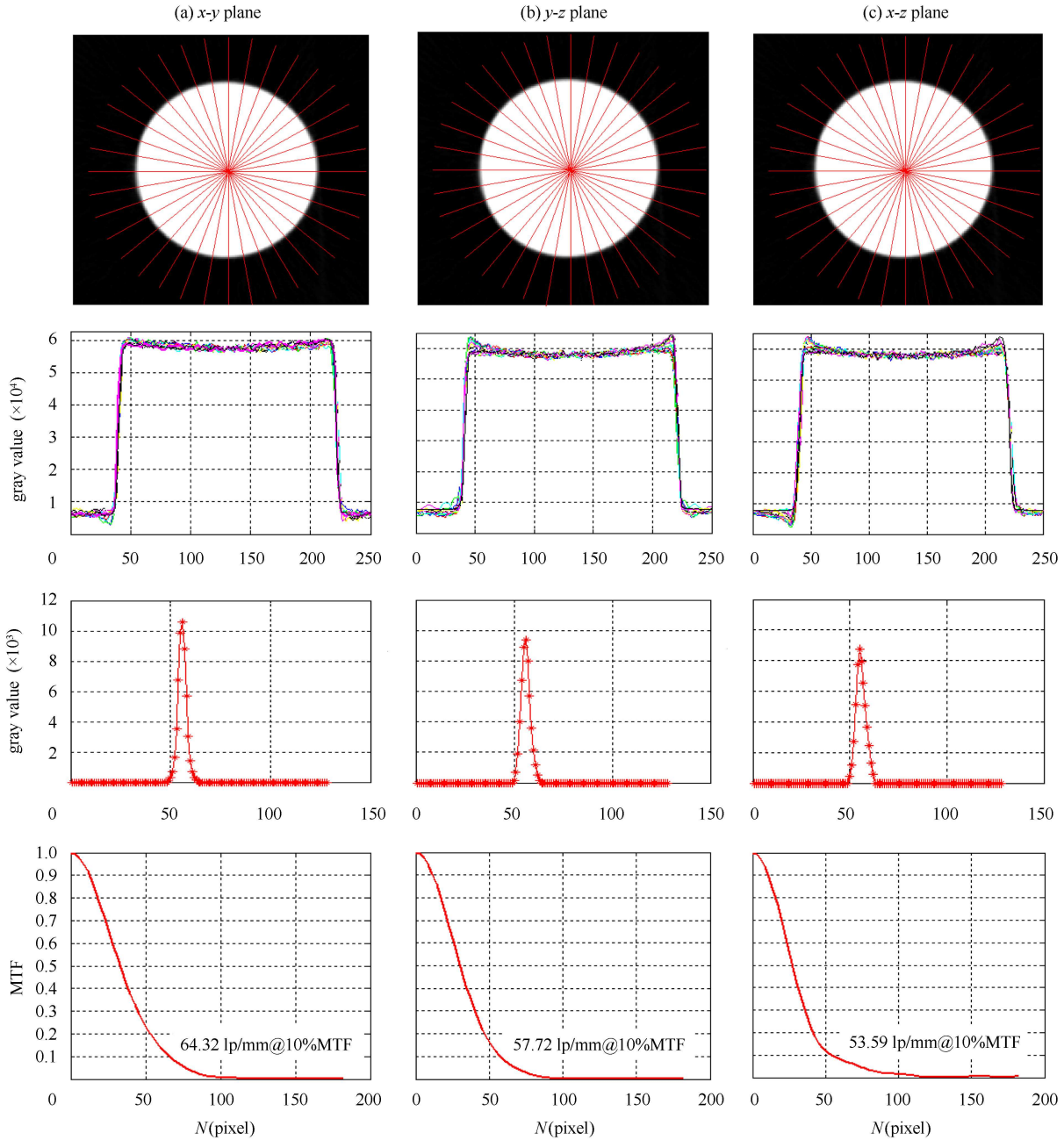


Fig. 10. The procedure of calculating the system PSF and MTF.

The relative non-roundness of the steel ball is 0.64% and has little influence on the measurement accuracy.

Data processing is as follows.

1) Extracting three orthogonal axial slices at the steel ball center: transaxial slice ( $x$ - $y$  plane:  $z=0$ ), coronal slice ( $x$ - $z$  plane:  $y=0$ ), sagittal slice ( $y$ - $z$  plane:  $x=0$ ).

2) Adding 18 sets of ERF profiles generated by radial scanlines with a  $10^\circ$  increment in each slice, the 2D PSF is the first derivative of the average ERF profile and the MTF is the modulus of the Fourier transformed 2D PSF. The procedure is shown in Fig. 10.

3) Adding 54 sets of ERF profiles generated by radial scanlines with a  $10^\circ$  increment in three orthogonal axial slices, the 3D PSF is the first derivative of the average ERF profile, the MTF which is the modulus of the Fourier transformed 3D PSF is regarded as the spatial resolution of the ICB $\mu$ CT system. The result is presented in Fig. 11.

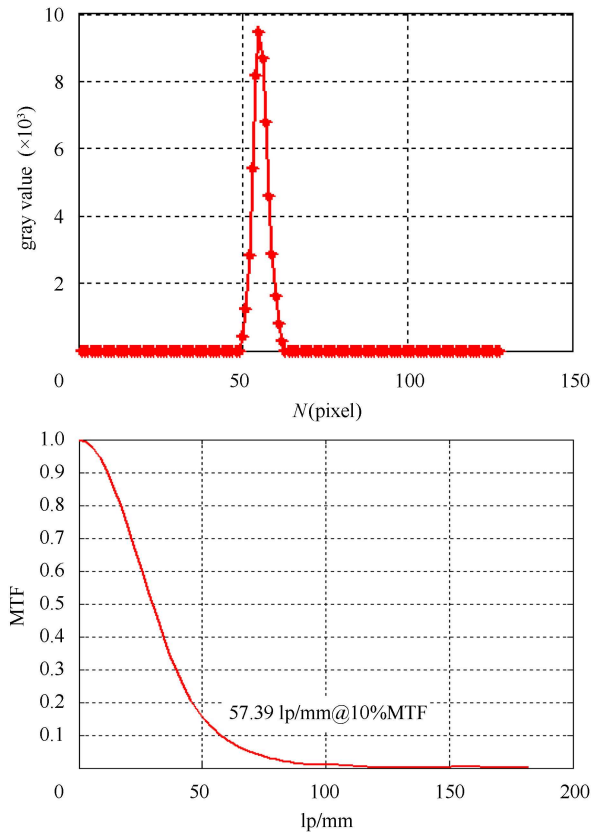


Fig. 11. The system PSF and MTF curve.

4) Generating 18 sets of ERF profiles that are different from the previous sampling, we repeat Step 2) and 3) twenty times. Then, the exact system spatial resolution (10% MTF value) and error level are given by Table 2, where lp is the abbreviation of the linepairs.

The MTFs in the three planes are different, since the

focal spot shape and the actual spatial resolution distribution in 3D space will affect the results.

### 3.2.2 Data processing of the density resolution measurement

We choose a PMMA uniform solid cylinder placed in the center of the mechanically turntable stage as the phantom to obtain 1800 projections by cone-beam  $\mu$ CT scanning in an optimal field. From the cone-beam CT images, we select a circular region with a diameter of about one third of the disc to one third extension in depth in order to extract a sub-cylinder which volume is about one third of the cylinder to measure. The measurement region is divided into equal size and non-overlapping block models. Each block model size range is from a single voxel to  $n$  voxels. Here  $n$  is equal to  $1 \times 1 \times 1$ ,  $3 \times 3 \times 3$ ,  $5 \times 5 \times 5$ ,  $7 \times 7 \times 7$ ,  $9 \times 9 \times 9$ ,  $11 \times 11 \times 11$ ,  $13 \times 13 \times 13$ ,  $15 \times 15 \times 15$ ,  $17 \times 17 \times 17$ ,  $19 \times 19 \times 19$ . We calculate the mean gray value within each block and the standard deviation to obtain the standard deviation in the mean. We express each standard deviation in the mean as a percent of its respective ensemble average and multiplied by a factor of 3 to obtain the CDF that actually is the density resolution in the 3D cone-beam  $\mu$ CT system. The detailed flow chart is shown in Fig. 12 and the CDF curve is plotted in Fig. 13. Table 3 depicts the CDF in different region sizes.

Table 2. The spatial resolution and error level.

	MTF(2D PSF)	MTF(3D PSF)
$x$ - $y$ plane	$(63.74 \pm 0.66)$ lp/mm	
$y$ - $z$ plane	$(57.62 \pm 0.55)$ lp/mm	
$x$ - $z$ plane	$(53.21 \pm 1.10)$ lp/mm	
$xyz$ space		$(55.56 \pm 0.56)$ lp/mm

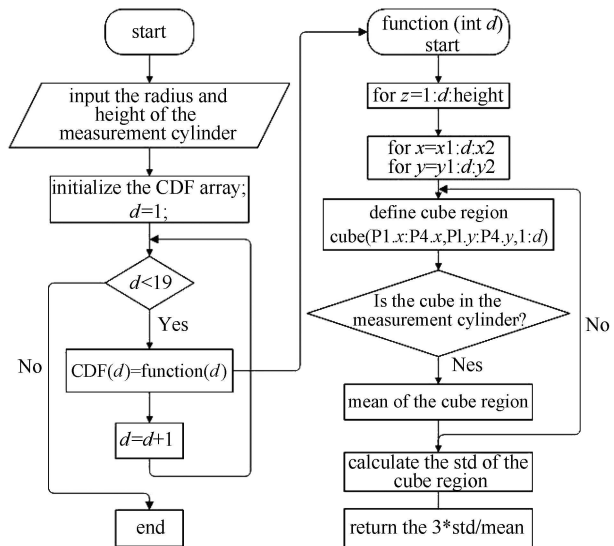


Fig. 12. The detailed flow chart to calculate the 3D CDF.

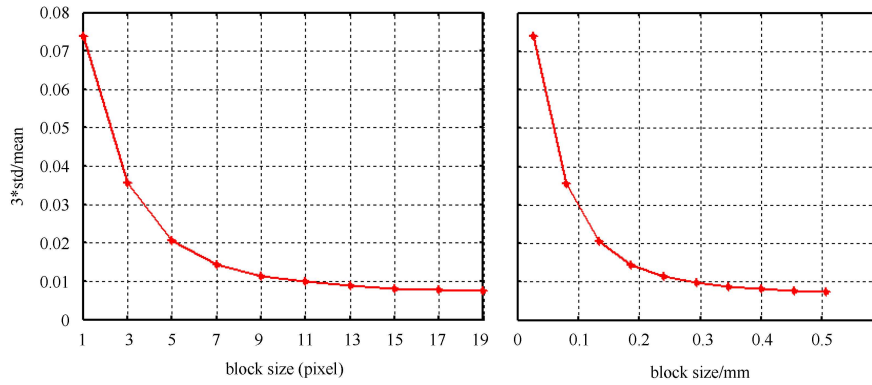


Fig. 13. The CDF curve plotted in logarithmic coordinates.

Table 3. The 3D CDF in different region size.

region unit/mm <sup>3</sup>	region unit (voxel)	3D CDF	region unit/mm <sup>3</sup>	region unit (voxel)	3D CDF
0.0267	1	7.40%	0.2937	11	0.99%
0.0801	3	3.55%	0.3471	13	0.88%
0.1335	5	2.06%	0.4005	15	0.82%
0.1869	7	1.44%	0.4539	17	0.78%
0.2403	9	1.14%	0.5073	19	0.75%

## 4 Conclusion and discussion

The ICB $\mu$ CT system is a genuine 3D imaging modality, the measurement of the system spatial resolution and the relative density resolution are very important. If we obtain the system spatial resolution by measuring the PSF of a point object directly, the point phantom (micro size and high precision) is very difficult to manufacture because of the higher resolution of the  $\mu$ m level in  $\mu$ CT system. Calculating the PSF indirectly by using the ERFs of the step edges is adopted in this paper. Due to the 3D PSF decomposition, the 3D PSF can be decomposed into three 2D PSFs at three orthogonal planes ( $x$ - $y$  plane,  $y$ - $z$  plane and  $x$ - $z$  plane), we utilize the 2D PSFs to describe the system 3D PSF. Our experimental result is  $(55.56 \pm 0.56)$  lp/mm. In this paper, we extend the measurement region from 2D to 3D to accurately obtain the relative density resolution of the 3D cone-beam  $\mu$ CT system. The experimental results figure out the 3D CDF in different region size, for example, the relative density resolution is 1% within  $300 \mu\text{m} \times 300 \mu\text{m} \times 300 \mu\text{m}$  according to the  $3\delta$  rule. The methods are simple and efficient. This paper introduces the measurement of the

system spatial resolution and relative density resolution, and furthermore, the results validate the performance index of the  $\mu$ CT system in our laboratory.

This paper mainly introduces a method to measure the 3D PSF and 3D CDF in the ICB $\mu$ CT system, there are still other issues involved in the paper which deserve to be researched deeply.

1) Strictly speaking, since the CT imaging system is a typical spatial shift-variant system, the PSF is different in different space positions, we assume local spatial invariance to measure the system 3D PSF. The anisotropic spatial resolution distribution of the ICB $\mu$ CT system needs intensive research.

2) Considering the limitation of the FDK algorithm, the different cone angle will affect the gray value. If non-central one third region of the cylinder is chosen to measure the relative density, the experimental result may be changed, which needs further study.

3) X-ray beam hardening artifacts in CT images will affect the spread of the edge function in 3D PSF and the gray value of the uniform cylinder in 3D CDF. The projection data used in this paper are based on beam hardening correction. The effect of beam hardening correction on 3D PSF and 3D CDF needs thorough research.

## References

- 1 CHEN Zi-Kuan, NING Ruo-La. Proc. of SPIE, 2007. 65100F
- 2 E1695-1995. American Society for Testing and Material(ASTM), 1995
- 3 GJB5311-2004, National Military Standard (NMS), 2004
- 4 CHEN Z K, NING R L. Phy. Med. Bio., 2004, 49(10): 1865-1880
- 5 YAN Yong-Lian, LIU Li, QUE Jie-Min et al. The Tenth. Conf. on NDT Tech., 2007. 56
- 6 CHEN Z K, NING R L, Conover D et al. Opt. Eng., 2006, 45(9): 97003-1-11
- 7 Van de Castele E, Van Dyck D, Sijbers J et al. Phy. Med. Ima., 2004, 5370: 2089-2096
- 8 La Feldkamp, Lc Davis, Jw Kress, J. Opt. Soc. Am. A, 1984, 1(6): 612-619
- 9 Canny J. IEEE Transactions on Pattern Analysis and Machine Intelligence, 1986, PAMI-8(6): 679-698